

Automated didactic prototype of pulmonary ventilation exhibits a simulation of intrathoracic pressure variations during diaphragmatic function

Protótipo didático automatizado de ventilação pulmonar exibe uma simulação de variações de pressão intratorácica durante a função diafragmática

Raphael José Pereira¹, Vitor Mainenti Leal Lopes², Rodrigo Hohl³,
Carlos Alberto Mourão-Júnior⁴, Akinori Cardozo Nagato⁵

Pereira RJ, Lopes VML, Hohl R, Mourão-Júnior CA, Nagato AC. Automated didactic prototype of pulmonary ventilation exhibits a simulation of intrathoracic pressure variations during diaphragmatic function / *Protótipo didático automatizado de ventilação pulmonar exibe uma simulação de variações de pressão intratorácica durante a função diafragmática*. Ver Med (São Paulo). 2022 Nov-Dec;101(6):2-196086.

ABSTRACT: The movement of air from the environment to the alveoli is a vital and complex phenomenon that occurs due to variations in intrathoracic and airway pressures in relation to the atmosphere. The construction of didactic prototypes can minimize the abstraction required in these *in vivo* phenomena. In this study, we automated a didactic prototype of pulmonary ventilation already described in literature to simulate and exhibit variations in intrathoracic pressure during diaphragmatic function. A pulmonary ventilation (PV) prototype was produced with recyclable materials, and automated by adapting a pressure sensor in the system to generate pressure curves as a function of time during the simulation of diaphragmatic function. The automated plunger's downward traction induced by the servomotor (such as diaphragmatic) reduced the pressure inside the bottle (intrathoracic), and this variation can be observed graphically on a computer interface while the balloon was expanded, and atmospheric air invaded its interior. *Conclusion:* The incorporation of technology into a simple PV prototype allowed a safe and simulated demonstration of how the diaphragm induces the variation of the intrathoracic pressure in relation to the atmosphere concomitantly with the pulmonary deformation that occurs during inspiration and exhalation.

RESUMO: O movimento do ar do ambiente para os alvéolos é um fenômeno vital e complexo que ocorre devido às variações nas pressões intratorácicas e nas vias aéreas em relação à atmosfera. A construção de protótipos didáticos pode minimizar a abstração necessária nestes fenômenos *in vivo*. Neste estudo, automatizamos um protótipo didático de ventilação pulmonar já descrito na literatura para simular e exibir variações na pressão intratorácica durante a função diafragmática. Um protótipo de ventilação pulmonar (PV) foi produzido com materiais recicláveis, e automatizado adaptando um sensor de pressão no sistema para gerar curvas de pressão em função do tempo durante a simulação da função diafragmática. A tração descendente do êmbolo automatizado induzida pelo servomotor (como o diafragmático) reduziu a pressão dentro da garrafa (intratorácica), e esta variação pode ser observada graficamente em uma interface de computador enquanto o balão foi expandido, e o ar atmosférico invadiu seu interior. *Conclusão:* A incorporação da tecnologia em um protótipo PV simples permitiu uma demonstração segura e simulada de como o diafragma induz a variação da pressão intratorácica em relação à atmosfera concomitantemente com a deformação pulmonar que ocorre durante a inspiração e a exalação.

Keywords: Prototype; Pulmonary; Ventilation; Thorax; Pressure.

Palavras-chave: Protótipo; Ventilação; Pulmonar; Tórax; Pressão.

1. Laboratory of Immunopathology and Experimental Pathology, Center for Reproductive Biology - CRB, Federal University of Juiz de Fora, Juiz de Fora, MG, Brazil. <https://orcid.org/0000-0001-8631-2731>. E-mail: raphaeljosepereira2013@gmail.com
 2. Depart. Production and Mechanical Engineering, Federal University of Juiz de Fora, Juiz de Fora, MG. <https://orcid.org/0000-0003-2168-4563>. E-mail: vmainenti@gmail.com
 3. Physiology Department, Federal University of Juiz de Fora, MG. <https://orcid.org/0000-0003-3194-9289>. E-mail: hohlrodrigo@gmail.com
 4. Physiology Department, Federal University of Juiz de Fora, MG. <https://orcid.org/0000-0001-7199-5365>. E-mail: camouraojr@gmail.com
 5. Physiology Department, Federal University of Juiz de Fora, Juiz de Fora, MG. Laboratory of Immunopathology and Experimental Pathology, Center for Reproductive Biology - CRB, Federal University of Juiz de Fora, MG. <https://orcid.org/0000-0002-7398-0834>. E-mail: akinori.nagato@ufjf.br
- Endereço para correspondência:** Akinori Cardozo Nagato. Laboratory of Immunopathology and Experimental Pathology, Center for Reproductive Biology - CRB, Federal University of Juiz de Fora, Juiz de Fora, MG, Brazil, Campus Universitário s/n, São Pedro. Postal code: 36036-900. E-mail: akinori.nagato@ufjf.br

INTRODUCTION

Respiratory mechanics is an area of science that seeks to explain chest and lung expansion under the action of muscular forces, and the resistance that these forces must overcome to move the air from the environment to the alveoli during inspiration or in the opposite direction during expiration. This vital and complex phenomenon is known as pulmonary ventilation (PV), and it occurs due to variations in intrathoracic and airway pressures in relation to the atmosphere¹.

PV can occur spontaneously (SPV) or artificially (APV). In SPV, the most important muscle is the diaphragm, a thin dome-shaped skeletal muscle membrane, located between the chest and abdomen, which by contracting increases the chest volume and generates sub-atmospheric pressure². In APV, the most recent models of artificial mechanical offer a volume of air under supra-atmospheric pressure in the airway direction at a flow rate (displacement of an air volume as a function of time) and programmable pressure³.

Advances in studies of SPV have historically accompanied the development of artificial mechanical ventilation (AMV), given the preliminary need for knowledge about SPV for a better understanding of integration of the respiratory system, and by extension the AMV^{4,5}. In the first half of the 20th century, the polio outbreak promoted advancement in this area, as it led to thousands of people using AMV as they were unable to ventilate their lungs spontaneously due to the gradual onset of induced acute respiratory failure (ARF), especially due to dysfunction of the diaphragm⁶. More recently, the pandemic caused by the SARS-CoV-2 virus (2019–2020) has led to increased production of mechanical ventilators (MV) due to the accelerated incidence of ARF in critically ill patients and the need for AMV⁷. In the latter case, the important points were the long time that patients remained on AMV and the difficulty of promoting integration of SPV and AMV. Thus, a careful review of basic and essential knowledge related to PV is required.

SPV is possible only because when the chest is immersed in an atmosphere, it expands its diameter under the action of driving forces induced by muscular action, especially by the diaphragm. In humans, the forced thoracic expansion is mainly done to the contraction of the diaphragm, which is lowered against the abdominal viscera, expanding the chest longitudinally and promoting the reduction of intrathoracic pressure (*i.e.*, *Boyle-Mariotte's Law*) and, concomitantly, pulmonary expansion. The displacement of air as a function of the time of thoracic expansion in the alveoli direction, is the result of the pressure gradient generated (greater in the atmosphere and less intrapulmonary) when the diameter of pulmonary alveoli concomitantly increases^{8,9,10,11} and the air overcomes the airway resistance.

To minimize the abstraction required in these *in vivo* phenomena, educators in different parts of the world have mobilized efforts in the construction of didactic prototypes especially since these phenomena are complex and *in vivo* observation is impractical. Furthermore, these prototypes reduce invasive studies with living beings and therefore, stand out for their ethical value^{12,13,14,15}.

The search for models that seek to clarify the phenomena observed in respiratory mechanics has been historically constant. In the field of respiratory physiology, Robert Hooke (1635–1703) is among the first authors to document a prototype to explain SPV from the sub-atmospheric pressure generated by a vacuum pump¹⁶. About a century and a half later, Hering's apparatus (1893)¹⁷ showed how the reduction of intrathoracic pressure concomitantly promoted PV and venous return to the heart¹⁸. Sherman¹⁹ incorporated a liquid into his prototype to demonstrate the pressure variation of pleural fluid during PV. Nagato et al.²⁰ presented essential biophysical concepts applied to SPV and APV using recyclable materials. Over the years, technology has been incorporated into new models. Balogh²¹ and Perchiazzi et al.²² sought to show the functioning of a mechanical ventilator through automated prototypes.

In this study, we automated a didactic prototype of pulmonary ventilation already described in literature to simulate and exhibit variations in intrathoracic pressure during diaphragmatic function²⁰. Minimalist prototypes that simulate pulmonary ventilation can serve to didactically present fundamental functions whose high abstraction in an integrated and complex system, as occurs in humans, are impaired.

MATERIAL AND METHODS

A PV prototype was produced with recyclable materials according to methods by Nagato et al.²⁰, and automated by adapting a pressure sensor in the system to generate pressure curves as a function of time during the simulation of diaphragmatic function.

Modeling the PV prototype

The prototype was built with a 250-ml bottle made of polyethylene terephthalate (PET) (chest wall), latex balloon (lung), and a 60-ml syringe (diaphragm muscle) (Figure 1A). The balloon was introduced into the bottle and fixed by elastic inversion. At the bottom of the bottle, a T-piece connector was placed to connect the syringe and the pressure sensor by a tube (Figure 1A). All materials were dimensioned in 3D modeling (*Software Computer Aided Design - CAD*). The static analysis of the materials was performed using the finite element method. Then, the prototype was automated.

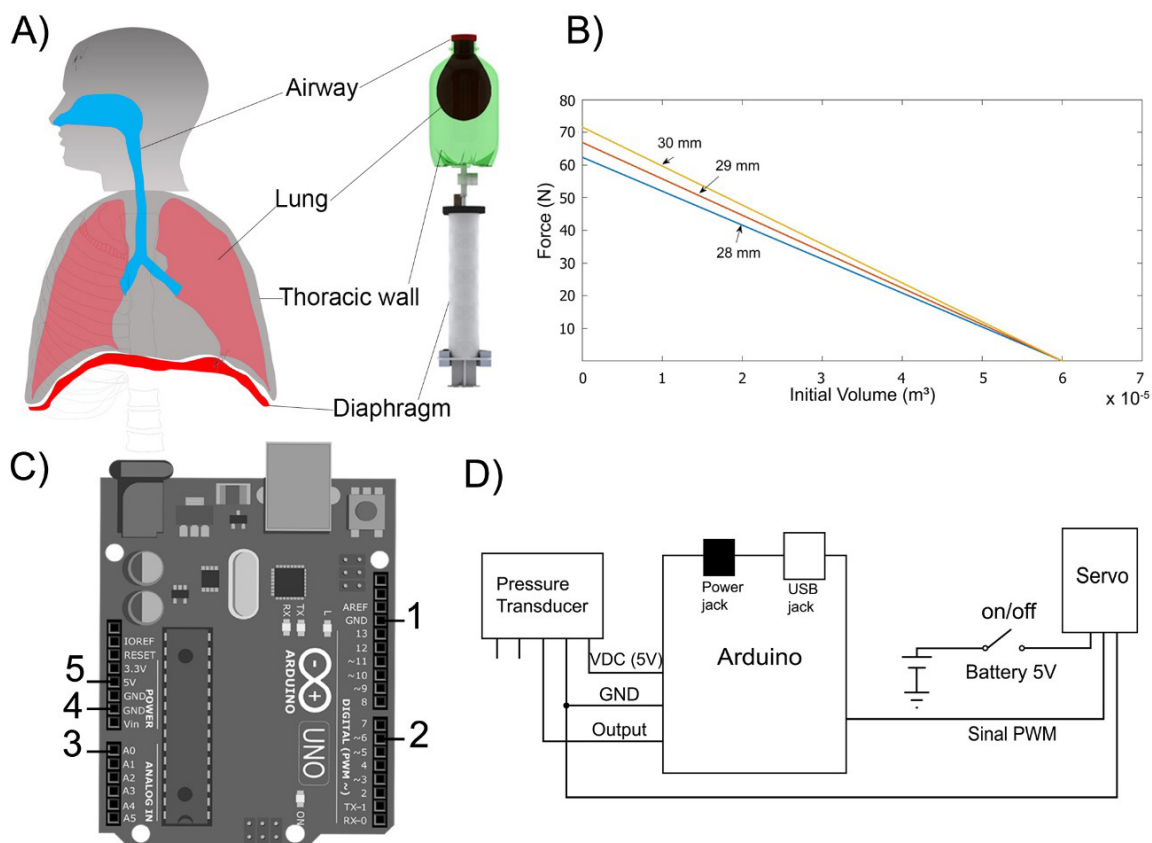


Figure 1 – Analogy between PV prototype and respiratory system (A). Force required to move the syringe tip according to the volume (B). Arduino uno (C). Schematic diagram of electric circuit (D). ‘A’ – Bottle made of polyethylene terephthalate (PET) of 250 ml (thoracic wall). Latex balloon (lung). Syringe of 60 ml (diaphragm). T-piece connector. B – ‘28’, ‘29’ and ‘30’ mm a syringe diameter. ‘C’ – Wire connections and PIN. 1 – servo (black or brown wire). 2 – servo (orange or yellow wire). 3 – Pressure transducer (output). 4 – Pressure transducer (GND). 5 – Pressure transducer (+5V). ‘D’ – Schematic diagram of electric circuit. VDC = Voltage Direct Current. GND = Ground. PWM = Pulse Width Modulation. USB = Universal Serial Bus.

Calculations for component design

For the dimensioning of the maximum charge to move plunger from 0 ml (zero) to 60 ml (maximum syringe volume), the system was closed and the Reynolds transport theorem was applied for the conservation of momentum, and expressed by Equation 1:

$$\frac{d}{dt}(B_{system}) = \frac{d}{dt} \left(\int_{CV} \beta \rho dV \right) + \left(\int_{CS} \beta \rho (\vec{v}_r \cdot \vec{n}) dA \right) \quad (1)$$

The variable B_{system} (Equation 2) is any property that depends on the amount of matter contained in the system (extensive property). $CVCV$ and $CSCS$ means volume control and control surface respectively. β is the derivative of property B_{system} with respect to mass (Equation 3). ρ is the specific mass. dV is the infinitesimal of volume. $\vec{v}_r \cdot \vec{v}_r$ is the relative velocity between the fluid flow velocity and the control volume

velocity and \vec{n} is the vector normal to the infinitesimal element of area (dA).

$$B_{system} = m \vec{v} \quad (2)$$

$$\frac{d}{dm}(B_{system}) = \beta = \vec{v} \quad (3)$$

Here m is the mass and \vec{v} is the fluid velocity in relation to an inertial frame.

Equation 1 was rewritten as follows (Equation 4):

$$\frac{d}{dt}(m\vec{v}) = \frac{d}{dt} \left(\int_{VC} \vec{v} \rho dV \right) + \left(\int_{VC} \vec{v} \rho (\vec{v}_r \cdot \vec{n}) dA \right) \quad (4)$$

The variation in the amount of momentum was expressed by the sum of the forces acting on the system and was represented by Equation 5:

$$\frac{d}{dt}(m\vec{v})_{system} = \sum \vec{F} \quad (5)$$

\vec{F} is equal to the vector sum of forces acting on

the control volume. The following simplifying hypotheses were considered: one-dimensional flow, incompressible flow ($\rho = \text{constant}$), and steady-state flow ($d/dt = 0$) simplified in Equation 6:

$$\sum \vec{F}_x = \left(\sum (\vec{v}\rho(\vec{v}\vec{n})A)_{\text{output}} - \sum (\vec{v}\rho(\vec{v}\vec{n})A)_{\text{input}} \right) \quad (6)$$

Considering that the system was closed, Equation 6 was rewritten as Equation 7:

$$\sum \vec{F}_x = 0 \quad (7)$$

Considering the force exerted by atmospheric pressure and the force required to remove the plunger from inertia as forces acting on the control volume, it was obtained (Equation 8):

$$\sum \vec{F}_x = F - p_{\text{atm}}A = 0 \quad (8)$$

As the result of Equation 8 was close to the value found when Boyle-Mariotte's Law (Equation 9) was applied, a rearrangement of the pressure definition was performed based on Equation 10:

$$P_1V_1 = P_2V_2 \quad (9)$$

$$F = \Delta PA \quad (10)$$

For the calculations and experimental tests, a 29-mm syringe was used. However, the analysis of forces required for 28- and 30-mm syringes was extrapolated (Fig. 1B) because of the lack of regularity of diameters in syringes by different manufacturers.

The volume of the tip syringe was considered 'initial volume,' (V_1) equaling $4.71 \times 10^{-8} \text{ m}^3$. The initial pressure (P_1) was equal to the atmospheric pressure, and the final volume (V_2) corresponded to (V_1) added to the displaced volume in the markings of syringe up to 60 mL. That is, (V_2) was equal to $6.00471 \times 10^{-5} \text{ m}^3$. Thus, the value calculated for the final pressure was $P_2 = 79.48 \text{ Pa}$. The estimated force (Equation 10) to move the plunger was equal to 66.87N.

Practical test of strength and critical work for the displacement of the plunger

The force to move the plunger was estimated by traction, with a closed system in relation to the atmosphere, simulating a critical working condition (Table 1). The initial load was 12.557N, corresponding to the added weight of the connectors and containers. Then, four loads were applied as shown in Table 1.

Table 1 - Critical work simulation through traction by using forces on the plunger

Charge	Value (kg)	Weight (N)
1 ^a	1.280	12.557
2 ^a	3.106	30.470
3 ^a	4.291	42.095
4 ^a	5.355	52.533
5 ^a	6.035	59.203

Note. For these tests the system were closed in relation to the atmosphere

Processed microcontroller

The automation was micro-controlled by an ATMEGA 328-Arduino processor (Figure 1C), model UNO R3 powered by USB or external adapter for 7 to 12 Vdc (Figure 1D), analog outputs, GND, 5-V output (for the pressure transducer), and pulse width modulation (PWM). Square waves were generated from PWM, representing the percentage of time in which there was a high logic level (Duty Cycle, stored in an 8-bit register, with a value from 0 = 0% to 255 = 100%). The percentage change was identified by the change in the average wave value, from 0V (0% duty cycle) to 5V (100% duty cycle). The programming structure of the micro processing was based on "C+" language, with the prior inclusion of a servo library with two functions being structured: 'setup' and 'loop.' There was no library for the pressure transducer; as only a direct reading was performed from the analog port.

Servomotor

A high torque servomotor (Hextronik HX12K), an electronic control system, and a potentiometer were connected to the output shaft to monitor the angle of the servo axis. The movement of the gears was limited from 0 ° to 180°. The signal was received by the servomotor (PWM) and reading was performed every 20ms. The detection of the change in pulse width was captured and the initial position of the potentiometer was checked. The control system was activated and the motor changed the position of the potentiometer to the position indicated by the pulse. To ensure maximum performance of the servo during the test, a higher torque was supplied, and to reduce the power loss, external power was used.

Pressure transducer

A piezoresistive differential pressure transducer (monolithic silicon, model MPX5700DP, 6.4 mV/kPa sensitivity) was connected (analog port) to the microcontroller to measure the pressure inside the bottle. The pressure was measured using an electrical signal generated by changing the resistance of the piezoresistive materials during the movement of the plunger. For

each Arduino reading interval (0 to 1023), the voltage was calculated using Equation 11. All calculations and commands on the Arduino platform were developed in 'C++' language. The initial reading reference was based on atmospheric pressure.

Prototype modeling

A compact, light, resistant, and easy-to-handle structure was digitally modeled using CAD Software - Solid Works, keeping the syringe-bottle structure in a vertical position for didactic purposes considering *Ortho statist* in the gravitational field.

Static analysis

Static analysis of the materials was conducted using the finite element method. The trajectory of the servomotor arm served as a starting point for the development of the structure in a medium-density fiberboard (MDF). The density of the MDF was determined from a specimen ($300 \times 14.5 \times 6\text{mm}$), with a mass of 22.9g , and the calculated value

was equals to 877.3946kg/m^3 . The elasticity module and internal adhesion were measured according to the principles described by Eleotério (2000)²³. In this way, the modulus of elasticity was adjusted to (5.881GPa) and internal adhesion (0.8229MPa).

The maximum moment provided by the servomotor (Figure 2A) was applied considering the restriction of arm displacement and critical mechanical situations. The force exerted by the servo and the physical and mechanical properties of the polypropylene syringe were as follows: specific weight = 0.91g/cm^3 , tensile yield strength of 35MPa, tensile strength at compression of 60MPa, elastic modulus of 100MPa, and Poisson's ratio of 0.4, the force transmitted from the servomotor arm to the syringe (Figure 2D), the reactions at the base of the syringe (Figure 2E), the support fixed to the syringe cylinder (Figure 2B), and a probable handling effort (Figure 2F). The syringe support rod was built considering the fixed base and the resulting moment of the servo arm (70N) applied to the front face of the rod (Figure 2C).

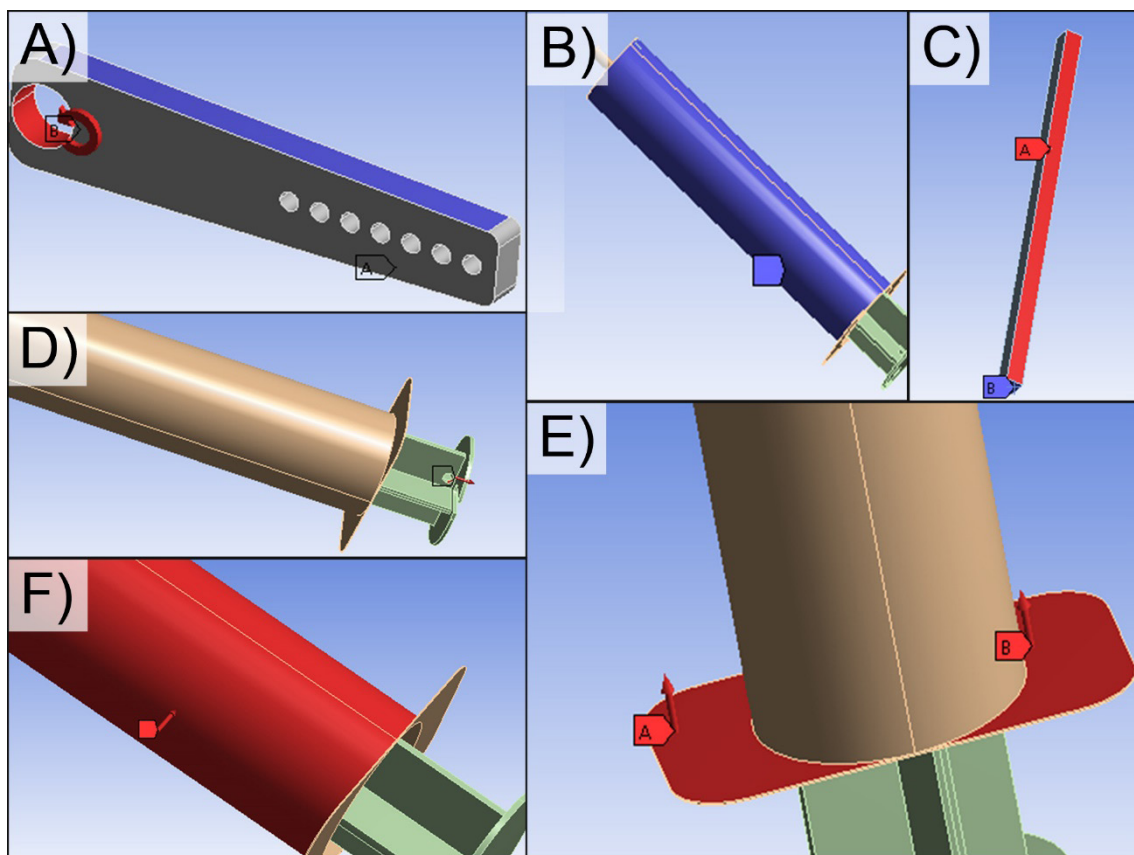


Figure 2 - Static force simulations or moment applied (red) and limit of displacement (blue) during prototype project. 'A' - critical movement restriction region in servomotor arm when applied a critical resulting moment (blue). 'B' - Syringe barrel. 'C' - contact forces between fixing claws and flange of syringe. 'D' - grip force estimated for prototype handling. (E) Critical region of contact force in hole edge for servomotor arm connection. (F) Syringe support arm.

Manufacture of support for prototype

(WS-10080 / 100 W / RDWorksV8 software) (Figure 3).

The cuts of the MDF pieces were made using a laser

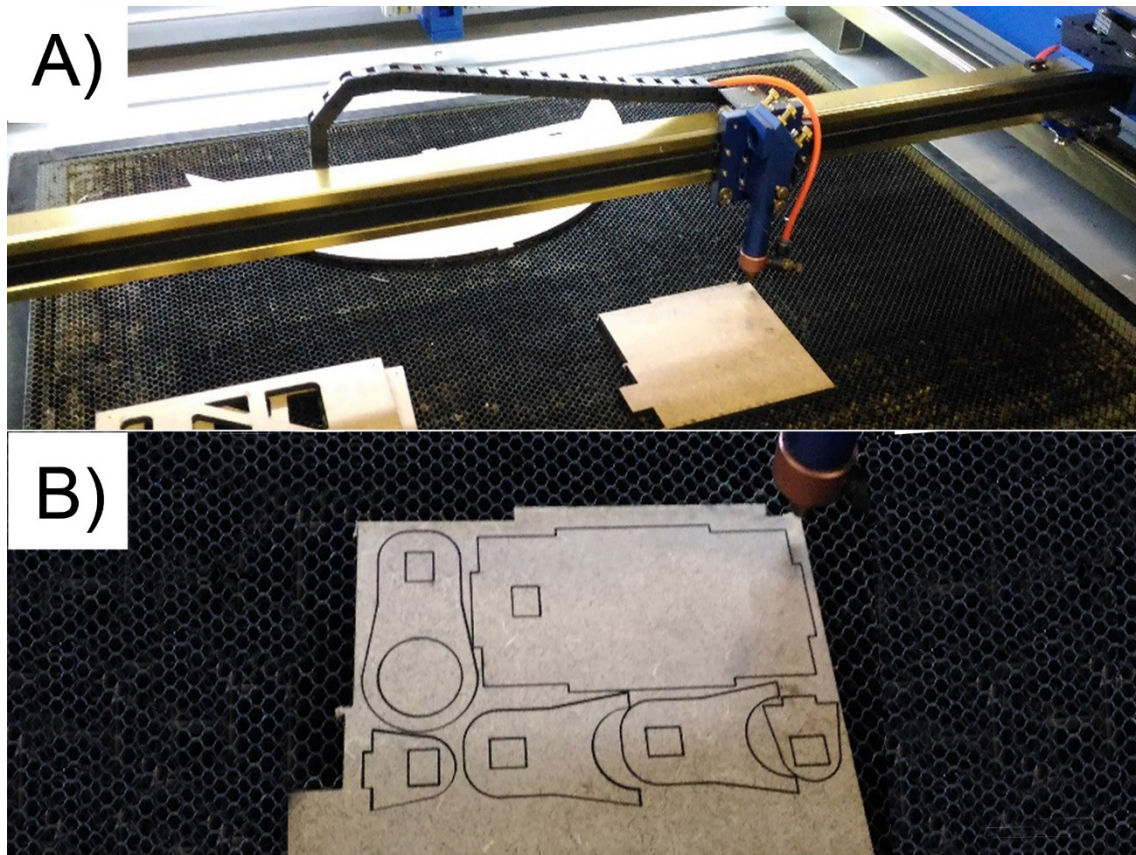


Figure 3 – Laser cutting of Medium-Density Fiberboard (MDF) structure. ‘A’ – MDF were positioned and the machine was configured for the cuts. ‘B’ - *MDF after cutting design.

Instrumentation and data analysis

The data were collected through the *Curve Fitting of MATrix LABoratory* (MATLAB) and generated codes exported to *Microsoft Excel*. The initial supply voltage was 4.9V, and the voltage for each reading was $L_v L_v$, calculated as follows (Equation 11):

$$L_v = \frac{4.9}{1024} = 0.004785 V^{(11)}$$

The reading performed by the Arduino Serial Plotter was displayed in real time and initially registered with an open system without connecting the pressure transducer to the system (Fig. 4A). The value fluctuated between 40 and 41. The upper limit was taken as a zero-reference point ($L_0 L_0$), and for the following calculations, Equation 12 was considered:

$$L_0 = 41 L_v = 0.1962 V^{(12)}$$

The values measured by Arduino were adjusted to reference mmHg (Equation 13), and the first curve was generated (Figure 4B).

$$pressao = \left(\frac{0.004785 L_l - L_0}{6400} \right) 7.5006^{(13)}$$

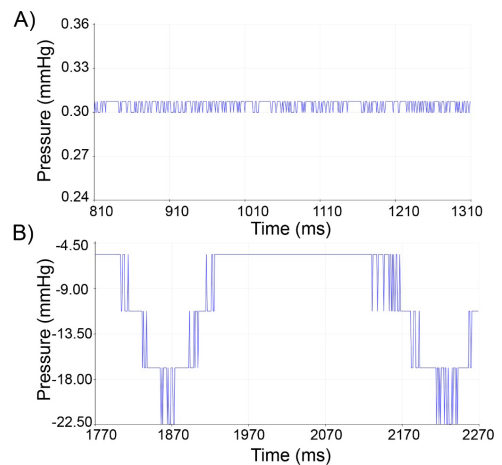


Figure 4 - Data collected with Arduino UNO and graphically registered. ‘A’ – reading performed at zero reference. ‘B’ – Curve of pressure (mmHg) during prototype function before data transformations in kPa.

Data file libraries were defined. For data storage, ‘s’ for ‘servomotor’, ‘pos’ for servomotor position, and ‘pressure’ for pressure values were considered. These commands are indicated in the setup function. The ‘s’ variable received the zero-reference position. The ‘loop’ was represented by the respiratory rate. The pressure values were recorded on the serial monitor or on the serial plot (command line Serial.println (pressure)).

The 10-ms time intervals for each degree shifted by the servomotor arm were determined from the ‘delay’ (10) command line. This mathematical modeling allowed an approximation of the data generated with the respiratory rates observed in humans (between 12 and 20 cycles/minute). For didactic purposes, the approximation of pressure values with those observed in the literature on the respiratory system was performed using the smoothing spline, sum of sites, and Fourier analysis (or transformed) methods.

RESULTS

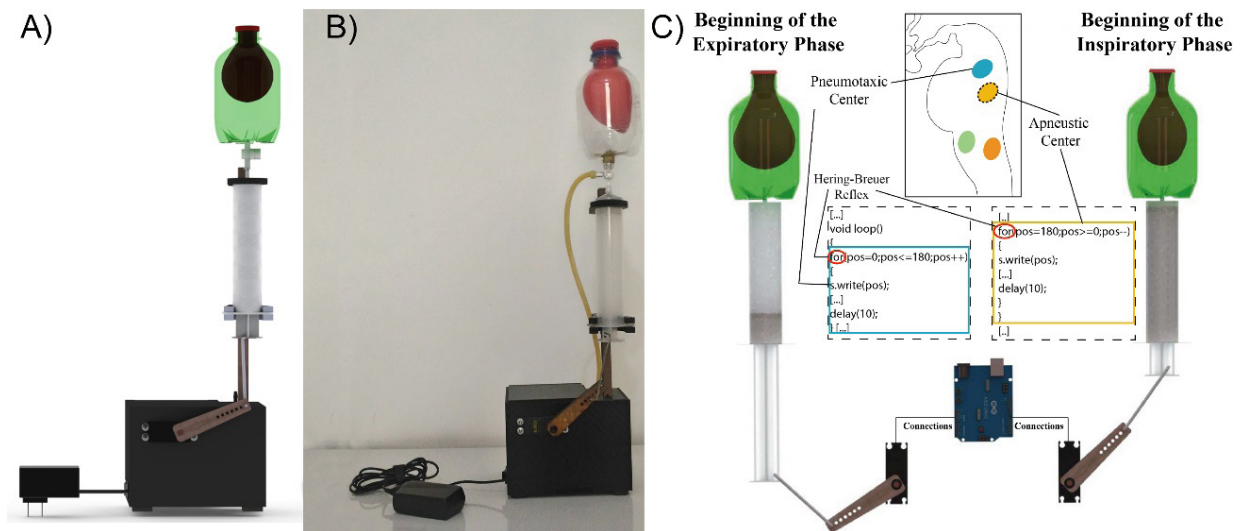


Figure 5 – ‘A’ – 3D Prototype design performed in *Software Computer Aided Design* (CAD). ‘B’ – Manufactured PV prototype. ‘C’ - Analogy between the Respiratory Center and Arduino executions in the prototype. Loop reading of the programming structures (blue and yellow rectangles) simulated the cyclical execution of the rate respiratory. The command ‘for’ (ellipse in red) allowed us to make an analogy with the Hering Breuer reflex. One of the programming structures (yellow rectangle) simulated the inspiration stimulus controlled by the apneustic center and the other programming structures (blue rectangle) simulated the action of the pneumotaxic center by inhibiting the inspiratory phase. Consecutive and alternating interruptions in the supply of the electrical signal, allowed to simulate the rate respiratory and observe the signals that start the expiratory phase (left prototype) and the inspiratory phase (right prototype) independently.

For example, the servomotor arm demonstrated a deformation of 3.5671 μm . (Figure 6 A). In the syringe, the point of greatest critical value of the deformation occurred in the region of force transmission from the servomotor to the syringe itself (Figure 6 C), while the critical point of

The vertical arrangement, ease of handling, absence of structural components that make the prototype’s observations polluted, and small final dimensional size were aspects that contributed to the feasibility of the automated prototype as a didactic tool (Figure 5 A, B). Generally, there was a low critical value for deformation and stress for all components of the prototype; demonstrating safety for its use and handling for educational purposes.

Another important aspect is the prototype’s potential to make an analogy between the functions of the respiratory center in controlling the respiratory rate with the executions performed by Arduino (Figure 5C). Through the *loop* reading of the programming structures, it was possible to simulate the cyclical execution of the respiratory rate. The ‘for’ command allowed us to make an analogy with the Hering-Breuer reflex. One of the programming structures simulated the stimulus for inspiration controlled by the apneustic center and the other simulated the action of the pneumotaxic center by inhibiting the inspiratory phase.

tension occurred in the region of contact with the clamping jaw (Figure 6 D). The highest critical deformation value (equal to 8.00 mm) was observed in the structural support rod (Figure 6 E) for the prototype to remain vertical.

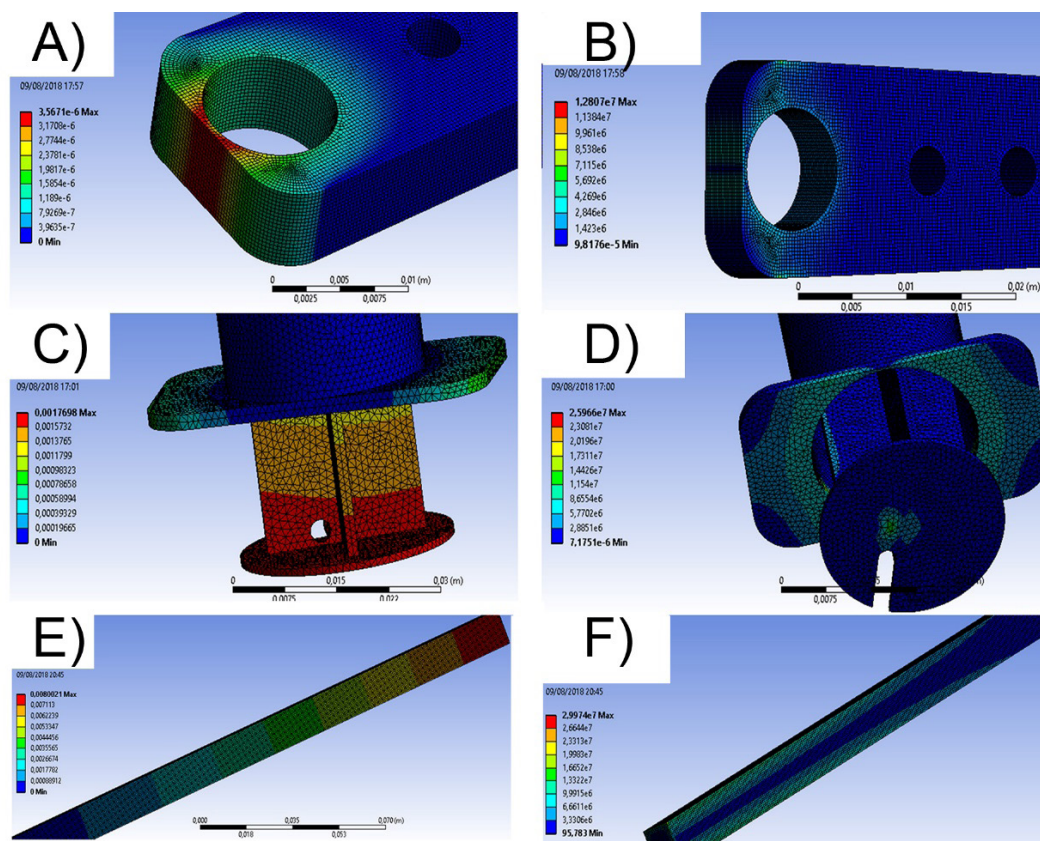


Figure 6 – Deformation and tension estimation using *Finite Element Method*. High critical value (red). Low critical value (blue). ‘A’ (deformation) and ‘B’ (tension) in servomotor arm. ‘C’ (deformation) and ‘D’ (tension) in syringe. ‘E’ (deformation in support end) and ‘F’ (tension in support base) in syringe support arm.

The integration of the pressure transducer in the prototype allowed dynamic demonstration of the pressure behavior inside the system (pleural space) and to qualitatively demonstrate the pressure variations inside the PET bottle (pleural space) for each variation of balloon volume (lung). We show the sinusoidal behavior of the pressure inside the bottle as a function of time (Figure 7).

Dynamically, the automated plunger traction downward induced by the servomotor (such as diaphragmatic mechanics during inspiration) reduced the pressure inside the bottle (intrathoracic), and this variation can be observed graphically on a computer interface (Figure 7) while the balloon was expanded, and atmospheric air invaded its interior. The return of the plunger to the initial position (event that represented the expiration) was accompanied by pressure increase, elastic retraction of the balloon, and exit of the air into the atmosphere. Interestingly, with the static system, it was also possible to demonstrate the sub-atmospheric pressure generated by the balloon’s own elastic retraction trend - a static trend of pulmonary collapse also observed *in vivo*.

DISCUSSION

There are different didactic prototypes in the literature related to SPV^{8,12} or APV²⁴. Generally, these

prototypes score in isolation, empirically, physical variables (such as strength, pressure, tension, shape, dimension, and positioning) that cannot be perceived directly at more complex and abstract levels of understanding *in vivo*^{8,25}. In this context, prototypes have been well regarded for generating new perspectives, promoting curiosity, objectivity, the development of applied reasoning²⁶, and the retention of knowledge²⁷.

John Mayow (1674)¹⁹ placed a balloon inside bellows (with a glass window) to observe the inflation and deflation of the bladder, and abstractly deduce the changes in pressure inside the bellows. Obviously, the lack of technology at the time did not allow analysis, interpretation, and graphic demonstrations to occur simultaneously with variations in pressure in the system.

In this study, we have advanced our knowledge especially through the incorporation of this technology, by incorporating a pressure sensor in a simple PV prototype, displaying clearly and instantly an isolated graphical interface with variations of intrathoracic pressure as a function of time, allowing the observation of the concomitant to balloon deformation. According to Chan et al.²⁸, these statements are valuable because during teaching, a lot of time is spent with passive and abstract instructions to demonstrate the relationship of these variables.

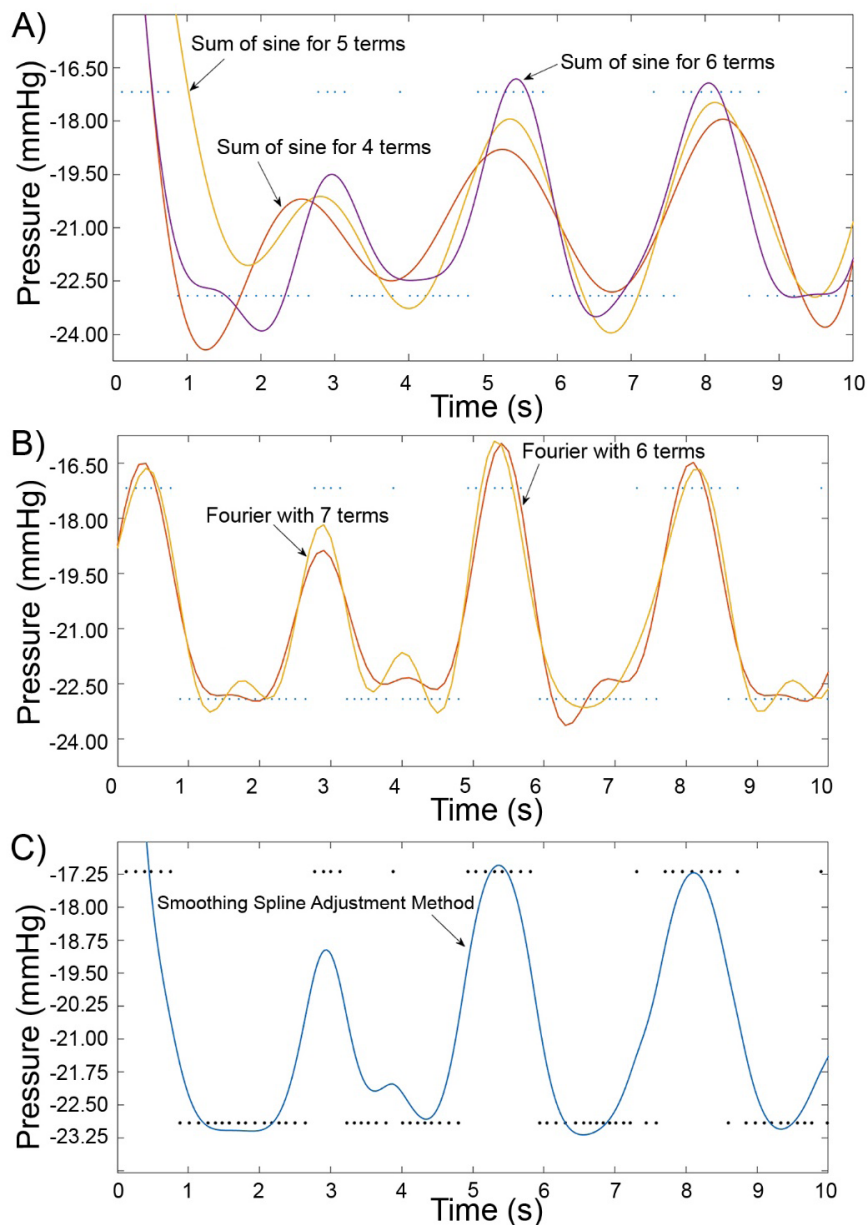


Figure 7 - Experimental pressure values interpolated through adjustment curves. 'A' - In each curve a points experimental approximation was applied by sum of sines. Four terms (red). Five terms (yellow). Six terms (purple). 'B' - Points experimental were adjusted by Fourier methods. Six terms (red). Seven terms (yellow). 'C' - Points experimental were adjusted by *Smoothing Spline*.

The automated prototype expanded the empirical possibilities of the allusions, allowing even more complex and specific discussions commonly discussed in the applied and related areas. The possibility of graduated control of the displacement force of the plunger, allowed discussion of respiratory muscle weakness (based on the reduction of the force generated by the servomotor) as a source factor, for example, for the inability of the respiratory pump to expand the lungs; a phenomenon that was also observed in type II respiratory failure *in vivo*²⁹. By disabling automation due to the absence of electrical current, for example, muscle weakness can be alluded to again, but it can also allude

to the need for the nervous system to trigger an electrical signal to control the diaphragmatic function³⁰.

Sherman¹⁹ developed a PV prototype in the presence of water between the balloon and container (representing the pleural fluid) and observed the pressure variation in the system similar to that in this study. Although we did not use liquid to represent pleural fluid in this study, we did not observe any loss in relation to the outcome of the study (the observation of pressure as a function of time, concomitantly with the expansion of the balloon). In addition, the presence of air, not liquid, has shown that even in the presence of air, keeping the system closed, it is still possible to have

some level of lung expansion. Respecting due proportions, this phenomenon is also observed *in vivo* when thoracic injuries occur and a small volume of atmospheric air and pleural fluid compete in the intrathoracic space (an event known as pneumothorax)³¹.

Recently, the functioning of PV was simulated from mathematical modeling demonstrating lung expansion from sub-atmospheric pressures induced by a vacuum pump³². The authors report the complexity of mathematically recreating lung tissue in their statements, and like this study; limited the model to the use of a rubber balloon replacing the lungs.

We see this limitation as an opportunity to discuss the replacement of the balloon by others of different densities, simulating lungs of different elastance and complacency, as occurs in diseases such as pulmonary fibrosis³³. Thus, it is possible to demonstrate the need to use a greater driving force to move the plunger, reduce intrathoracic pressure, and promote the same level of expansion among balloons.

In this study, a low-resistance balloon was initially used. However, when a more resistant balloon was tested, and the plunger (diaphragm) was displaced, the walls of the bottle concentrically deformed toward the balloon before the balloon expanded. Interestingly, this helped to explain another phenomenon observed *in vivo* (clinically) defined as ‘paradoxical movement.’ In humans, this mechanism occurs when there is diaphragmatic weakness and the chest expansion depends predominantly on other muscles. When this occurs, the accessory muscles contract by raising the ribs and briefly expanding the chest. Even before expansion occurs, the anatomical structures offering low resistance are concentrated concentrically (intercostal and abdominal region), exhibiting a depression of the skin that can be seen with the naked eye³⁴.

We speculate that future improvement of the prototype, for example, by modifying the resistance imposed to the passage of air, can help explain the need for increased diaphragmatic biomechanical work to move air in the airways. From a didactic perspective, these new paths can provide a basis for discussing other biophysical foundations such as aspects related to *Poiseuille’s Law*, and

clinical aspects similar to those that occur in obstructive diseases such as asthma.

There is evidence that the use of active learning strategies improves performance in respiratory physiology²⁵. In this sense, we suggest that it is evaluated whether the developed prototype increases student involvement and modifies academic performance. We believe in the didactic potential of this type of technology used as a tool to foster discussions, support, improve, and update the teaching on respiratory mechanics.

The prototype holds in itself didactic concepts that can also be explored through handling, when it is not automated and the pressure detection system is disconnected from the prototype. When handling it, it is possible to perceive, for example, the force used to promote the expansion of the latex ball (“the lungs”). The familiarity in handling broadens the possibility of discussion about the knowledge applied to biophysics, physiology and respiratory pathophysiology, and even the principles about artificial mechanical ventilation. It is possible to foster wide-ranging discussions about: the variation of thoracic pressure as a function of respiratory muscle strength (“syringe plunger”); the variation of thoracic pressure in cases of pneumothorax (communication between the atmosphere and the internal space of the bottle); the variation of thoracic pressure as a function of the elastic properties of the lungs (“latex ball”). Together, the demonstration of the pressure variation incorporated into the technology, added to the empirical observations of its handling, improve the prototype as a didactic tool and aid and educator in teaching about the knowledge surrounding the respiratory pump.

CONCLUSION

The incorporation of technology into a simple PV prototype allowed a safe and simulated demonstration of how the diaphragm induces the variation of the intrathoracic pressure in relation to the atmosphere concomitantly with the pulmonary deformation during inspiration and exhalation.

Authors contributions: R.J.P., V.M.L.L., and A.C.N. conceived and designed the research and executed the study including the prototype scripts for model building and the prototype workflows for data handling; R.J.P. and A.C.N. performed experiments. R.J.P., V.M.L.L., and A.C.N. analyzed data; R.J.P., A.C.N., R.H., and C.A.M.J. interpreted the results of experiments; R.J.P. prepared figures; R.J.P., R.H., C.A.M.J., and A.C.N. drafted manuscript; R.J.P., A.C.N., R.H., C.A.M.J. revised manuscript; A.C.N. edited manuscript. All authors have read and approved the final manuscript.

Acknowledgments: We are very grateful to Antônio Alencar Nogueira Pancoti and Filipe Augusto Pires for her skillful technical assistance during the experiments at the Robotics Laboratory Juiz de Fora Federal University. (LABRA).

Funding: This study was supported by the Aerodesign Project of Juiz de Fora Federal University.

Disclosures/Conflicts: The authors declare that they have no competing interests.

Availability of data and materials: Data sharing is not applicable to this article as no datasets were generated or analyzed during the current study.

REFERENCES

1. West JB. History of respiratory mechanics prior to World War II. *Compr Physiol*. 2012;2(1):609-619. doi: <https://doi.org/10.1002/cphy.c080112>
2. West JB. Leonardo da Vinci: engineer, bioengineer, anatomist, and artist. *Am J Physiol Lung Cell Mol Physiol*. 2017;312(3):L392-L397. doi: <https://doi.org/10.1152/ajplung.00378.2016>
3. Slutsky AS. History of mechanical ventilation. From Vesalius to ventilator-induced lung injury. *Am J Respir Crit Care Med*. 2015;191(10):1106-1115. doi: <https://doi.org/10.1164/rccm.201503-0421PP>
4. Aoki N, Shimizu H, Kushiyama S, Katsuya H, Isa T. A new device for synchronized intermittent mandatory ventilation. *Anesthesiology*. 1978;48(1):69-71. doi: <https://doi.org/10.1097/0000542-197801000-000095>.
5. Koutsoukou A, Perraki H, Orfanos SE, et al. History of mechanical ventilation may affect respiratory mechanics evolution in acute respiratory distress syndrome. *J Crit Care*. 2009;24(4):e621-626. doi: <https://doi.org/10.1016/j.jcrc.2009.02.003>
6. West JB. The physiological challenges of the 1952 Copenhagen poliomyelitis epidemic and a renaissance in clinical respiratory physiology. *J Appl Physiol*. 2005;99(2):424-432. doi: <https://doi.org/10.1152/jappphysiol.00184.2005>
7. Ranney ML, Griffeth V, Jha AK. Critical supply shortages - the need for ventilators and personal protective equipment during the Covid-19 pandemic. *N Engl J Med*. 2020;382(18):e41. doi: <https://doi.org/10.1056/NEJMp2006141>
8. Chan V, Pisegna J, Rosian R, DiCarlo SE. Model demonstrating respiratory mechanics for high school students *Am J Physiol*. 1996 Jun;270(6 Pt 3):S1-18. doi: [10.1152/advances.1996.270.6.S1](https://doi.org/10.1152/advances.1996.270.6.S1). Erratum in: *Am J Physiol* 1997 Jun;272(6 Pt 3):followi. doi: <https://doi.org/10.1152/advances.1996.270.6.S1>
9. San Bok J, Lee GD, Kim DK, Lim D, Joo SK, Choi S. Changes of pleural pressure after thoracic surgery. *J Thorac Dis*. 2018;10(7):4109-4117. doi: <https://doi.org/10.21037/jtd.2018.06.131>
10. Sircar S. A simple device for measuring static compliance of lung-thorax combine. *Adv Physiol Educ*. 2015;39(3):187-188. doi: <https://doi.org/10.1152/advan.00026.2014>
11. Wilson TA, De Troyer A. Diagrammatic analysis of the respiratory action of the diaphragm. *J Appl Physiol*. 2010;108:251-255. doi: <https://doi.org/10.1152/jappphysiol.00960.2009>
12. Anderson J, Goplen C, Murray L, et al. Human respiratory mechanics demonstration model. *Adv Physiol Educ*. 2009;33(1):53-59. doi: <https://doi.org/10.1152/advan.90177.2008>
13. Ratnovsky A, Elad D, Halpern P. Mechanics of respiratory muscles. *Respir Physiol Neurobiol*. 2008;163(1-3):82-89. doi: <https://doi.org/10.1016/j.resp.2008.04.019>
14. Rosen KR, McBride JM, Drake RL. The use of simulation in medical education to enhance students' understanding of basic sciences. *Med Teach*. 2009;31(9):842-846. doi: <https://doi.org/10.1080/01421590903049822>
15. Zhang XY. Biomedical engineering for health research and development. *Eur Rev Med Pharmacol Sci*. 2015;19(2):220-224.
16. West JB. Robert Hooke: early respiratory physiologist, polymath, and mechanical genius. *Physiology (Bethesda)*. 2014;29(4):222-233. doi: <https://doi.org/10.1152/physiol.00005.2014>
17. Rothe R. Lunge. Specialitäten physiologischer Apparate: preliminary catalog. Prag: Hofbuchdruckerei A Haase; 1893. (Collection Rand B Evans).
18. Magder S. Heart-Lung interaction in spontaneous breathing subjects: the basics. *Ann Transl Med*. 2018;6(18):348. doi: <https://doi.org/10.21037/atm.2018.06.19>
19. Sherman TF. A simple analogue of lung mechanics. *Am J Physiol*. 1993;265(6Pt3):S32-34. doi: <https://doi.org/10.1152/advances.1993.265.6.S32>
20. Nagato ACDM, Bandeira ACB, Bezerra FS. Protótipo de ventilação mecânica espontânea e artificial. *Rev Saude Publica*. 2012;5(3):495-500. Disponível em: <https://periodicos.unicesumar.edu.br/index.php/saudpesq/article/view/2453/1806>
21. Balogh R. Educational Robotic Platform based on Arduino. 2010. Available from: https://www.researchgate.net/publication/228379484_Educational_Robotic_Platform_based_on_Arduino
22. Perchiuzzi G, Rylander C, Pellegrini M, Larsson A, Hedenstierna G. Robustness of two different methods of monitoring respiratory system compliance during mechanical ventilation. *Med Biol Eng Comput*. 2017;55(10):1819-1828. doi: <https://doi.org/10.1007/s11517-017-1631-0>.
23. Eleotério, Jackson Roberto. Propriedades físicas e mecânicas de painéis MDF de diferentes densidades e teores de resina [dissertação]. Piracicaba: Universidade de São Paulo, Escola Superior de Agricultura Luiz de Queiroz; 2000 [citado 28 nov. 2022]. doi: <https://doi.org/10.11606/D.11.2000.tde-18102002-164850>
24. Al Hussein AM, Lee HJ, Negrete J, et al. Design and prototyping of a low-cost portable mechanical ventilator. *J Med Devices*. 2010;4(2):027514. doi: <https://doi.org/10.1115/1.3442790>
25. Rao SP, and DiCarlo SE. Active learning of respiratory physiology improves performance on respiratory physiology examinations. *Adv Physiol Educ*. 2001;25(2):55-61. doi: <https://doi.org/10.1152/advances.2001.25.2.55>
26. Rodenbaugh DW, Collins HL, Chen CY, DiCarlo SE.

- Construction of a model demonstrating cardiovascular principles. *Am J Physiol*. 1999;277(6 Pt 2):S67-83. doi: <https://doi.org/10.1152/advances.1999.277.6.S67>
27. DiCarlo SE. Teaching alveolar ventilation with simple, inexpensive models. *Adv Physiol Educ*. 2008;32(3):185-191. doi: <https://doi.org/10.1152/advan.90156.2008>
28. Giuliadori MJ, DiCarlo SE. Simple, inexpensive model spirometer for understanding ventilation volumes. *Adv Physiol Educ*. 2004;28(1-4):33. doi: <https://doi.org/10.1152/advan.00034.2003>
29. Roussos C, Koutsoukou A. Respiratory failure. *Eur Respir J Suppl*. 2003;47:3s-14s. doi: <https://doi.org/10.1183/09031936.03.00038503>
30. Dube BP, Dres M. Diaphragm dysfunction: diagnostic approaches and management strategies. *J Clin Med*. 2016;5(12):113. doi: <https://doi.org/10.3390/jcm5120113>
31. Brims FJ, Maskell NA. Ambulatory treatment in the management of pneumothorax: a systematic review of the literature. *Thorax*. 2013;68(7):664-669. doi: <https://doi.org/10.1136/thoraxjnl-2012-202875>
32. Šolc F, Veselý I, Sekora J, Mézl M, Eschli A, Provazník I. The mathematical model of a LUNG simulator. *Mefanet J*. 2014;2(2):71-78. Available from: <http://mj.mefanet.cz/mj-04141203>
33. West JR, Alexander JK. Studies on respiratory mechanics and the work of breathing in pulmonary fibrosis. *Am J Med*. 1959;27:529-544. doi: [https://doi.org/10.1016/0002-9343\(59\)90038-5](https://doi.org/10.1016/0002-9343(59)90038-5)
34. Maloney JV Jr, Schmutzer KJ, Raschke E. Paradoxical respiration and "pendelluft". *J Thorac Cardiovasc Surg*. 1961;41:291-298.

Received: March 29, 2022

Accepted: September 26, 2022